Energy transfer in LHCII monomers at 77K studied by sub-picosecond transient absorption spectroscopy.

Kleima, F.J.; Gradinaru, C.C.; Calkoen, F.; van Stokkum, I.H.M.; van Grondelle, R.; van Amerongen, H.

published in
Biochemistry
1997

DOI (link to publisher)
10.1021/bi9716480

document version
Publisher's PDF, also known as Version of record

Energy Transfer in LHCII Monomers at 77K Studied by Sub-Picosecond Transient Absorption Spectroscopy

Foske J. Kleima,* Claudiu C. Gradinaru, Florentine Calkoen, Ivo H. M. van Stokkum, Rienk van Grondelle, and Herbert van Amerongen

Department of Physics and Astronomy and Institute for Condensed Matter and Optical Physics, Vrije Universiteit Amsterdam, De Boelelaan 1081, 1081 HV Amsterdam

Received July 9, 1997; Revised Manuscript Received October 1, 1997[⊗]

ABSTRACT: Energy transfer from chlorophyll *b* (Chl *b*) to chlorophyll *a* (Chl *a*) in monomeric preparations of light-harvesting complex II (LHCII) from spinach was studied at 77 K using pump−probe experiments. Sub-picosecond excitation pulses centered at 650 nm were used to excite preferentially Chl *b* and difference absorption spectra were detected from 630 to 700 nm. Two distinct Chl *b* to Chl *a* transfer times, ∼200 fs and 3 ps, were found. A clearly distinguishable energy transfer process between Chl *a* molecules occurred with a time constant of 18 ps. The LHCII monomer data are compared to previously obtained LHCII trimer data, and both data sets are fitted simultaneously using a global analysis fitting routine. Both sets could be described with the following time constants: 140 fs, 600 fs, 8 ps, 20 ps, and 2.9 ns. In both monomers and trimers 50% of the Chl *b* to Chl *a* transfer is ultrafast (<200 fs). However, for monomers this transfer occurs to Chl *a* molecules that absorb significantly more toward shorter wavelengths than for trimers. Part of the transfer from Chl *b* to Chl *a* that occurs with a time constant of 600 fs in trimers is slowed down to several picoseconds in monomers. However, it is argued that observed differences between monomers and trimers should be ascribed to the loss of some Chl *a* upon monomerization or a shift of the absorption maximum of one or several Chl *a* molecules. It is concluded that Chl *b* to Chl *a* transfer occurs only within monomeric subunits of the trimers and not between different subunits.

Light-harvesting complex II (LHCII)[1] is the most abundant light-harvesting antenna pigment−protein complex of green plants. In nature it is believed to be organized in trimeric units and it binds 50% of the chlorophyll (CHl) present in the chloroplast (*1*). HPLC analysis has shown that each monomeric subunit binds 5−6 Chl *b*, 7−8 Chl *a*, and several xanthophyll (Xan) molecules: 2 luteins (Lut), 1 neoxanthin (Neo), and varying, substoichiometric amounts of violaxanthin (Vio) [see also Table 1, which is taken from (*2*)].

The structure of the trimeric LHCII has been resolved to 3.4 Å using electron microscopy and electron diffraction of two-dimensional crystals (*3*). A significant part of the 26 kDa monomeric LHCII protein and the positions of 12 Chls and two luteins in the center of the protein were determined. However, the resolution was not high enough to distinguish between Chl *a* and Chl *b*, and the orientation of the lowest-energy electronic transition dipole moment (Q_y) of the individual chlorophylls cannot yet be assigned. Center to center distances between Chl *a* and Chl *b* within a monomer range from 8.3 to 10.5 Å. The role of the xanthophylls is, apart from light harvesting and structural stabilization of the complex, to quench Chl triplets to prevent the formation of singlet oxygen. This is only possible when the distance between the Chls and the Xans is small (*4*). On the basis of the idea that excitons are transferred very fast from Chl *b* to Chl *a*, so that Chl triplets are only formed on Chl *a*, a preliminary assignment of the chlorophyll identities was made: the seven molecules closest to the luteins were proposed to be Chl *a*, and the five remaining chlorophylls were assigned to Chl *b* (*3*). However, it is known that other carotenoids also play a role in triplet quenching, thereby challenging the reasoning behind the assignment (*5*−*7*). Another problem is the fact that not all pigments that are bound to the protein, according to the HPLC data, can be localized in the crystal structure.

Table 1: HPLC Pigment Analysis of Trimeric and Monomeric LHCII Prepared Using Phospholipase (*2*) (Number of Chl *b* Molecules Normalized to 6 per Monomer)

sample	Chl *a*	Chl *b*	Lut	Neo	Vio
trimers	8.28 ± 0.3	6	2.20 ± 0.2	1.10 ± 0.16	0.26 ± 0.03
monomers	6.84 ± 0.24	6	2.16 ± 0.14	0.92 ± 0.13	0.09 + 0.02

Trimeric LHC II has been studied extensively using both steady-state (*8*−*11*) and time-resolved spectroscopy (*12*−*21*). Whereas only two main absorption bands in the 640−700 nm region are observed at room temperature, as many as 6−9 bands were observed in absorption, circular dichroism, and linear dichroism spectra at 77 K (*8*), and today the spectral fingerprint consists of eleven features (*11*). Several earlier (sub)picosecond spectroscopic studies focusing on Chl *b* to Chl *a* energy transfer have been performed on LHCII trimers (*15*−*20*). Transfer times found in these studies ranged from 100 to 600 fs and also transfer times on the

† This work has been supported by the Dutch Science Foundation (FOM) and the Human Frontier Science Program Organisation (HFSPO), Grant 1932802.

* Address correspondence to this author. Telephone: +31 20 444 7941. Fax: +31 20 444 7899. E-mail: foske@nat.vu.nl.

⊗ Abstract published in *Advance ACS Abstracts,* November 15, 1997.

[1] Abbreviations: Chl, chlorophyll; LHCII, light-harvesting complex II; Xan, Xanthophyll; Lut, lutein; Neo, neoxanthin; Vio, violaxanthin; plA_2, phospholipase A_2; w/v, weight per volume; v/v, volume per volume, ΔOD spectrum, absorption difference spectrum; DADS, decay-associated difference spectra; SADS, species-associated difference spectra.

S0006-2960(97)01648-6 CCC: $14.00

picosecond time scale were reported. A 77 K study performed in our lab yielded three distinct Chl *b* to Chl *a* transfer times: <300 fs, 600 fs, and 4−9 ps. "Slow" energy transfer (10−20 ps) was observed between some of the Chl *a* molecules. Transfer between different monomers in a trimer was suggested to occur on a similar time scale (10−20 ps) (*12*). Recently, an essentially annihilation free study (*13*) at room temperature appeared with results that were in good agreement with our results (*12*) yielding transfer times of 175 fs, 625 fs, and 5 ps (*13*). In addition, two components with lifetimes of 34 and 85 ps were found with very low amplitudes and a nondecaying component (3.6 ns) (*13*). Since the identity of the Chl pigments was not resolved in the crystal structure (*3*), it is not known between which pigments in the structure the Chl *b* to Chl *a* transfer occurs.

Starting from the Kühlbrandt assignment some model calculations based on Förster energy transfer have been performed (*12*). These simulations suggested that the Chl *b* to Chl *a* transfer processes mainly occured in Chl *a*−Chl *b* pairs within the monomer, implying that Chl *b* to Chl *a* transfer times in monomers and trimers would be essentially the same. These calculations were performed under the assumption that the chlorophyll assignment in (*3*) is correct. Using similar Förster transfer calculations as in (*12*), with a reasonable choice of the refractive index of 1.5, one can easily verify that Chl *b* to Chl *a* energy transfer between pigments on different monomers would take at least several picoseconds, regardless of the assignment of the pigment identities. We found in (*12*) that approximately 80% of the Chl *b* excitations are transferred to Chl *a* with a transfer time of 600 fs or faster, and only 20% in several picoseconds. Therefore, the major part of the Chl *b* to Chl *a* transfer occurs within the monomeric subunits but the picosecond component might in principle be due to intermonomeric energy transfer. In order to test whether this transfer step is intra- or inter-monomeric, we performed sub-picosecond transient absorption measurements on monomeric LHCII.

It has been shown before that it is possible to form monomers from LHCII trimers from spinach using a phospholipase treatment in high detergent concentrations (*11*). The pigment composition of these monomers is not entirely the same as the composition of the trimers [see Table 1 (*2*)]. Approximately 1−2 Chl *a* molecules (per monomer) are lost together with some Vio, which is not resolved in the LHCII structure (*3*). The monomer complexes were studied by steady-state spectroscopy and compared to trimeric LHCII data (*11*). The global spectral features are to a large extent similar for monomers and trimers, but, on the basis of CD measurements, it was argued that exciton interactions between two Chl *a* molecules and two Chl *b* molecules are lost upon monomerization (*11*).

We will show in this paper that despite the handicap that the monomeric preparations have lost some Chl *a*, which complicates the interpretation of the results, it can be concluded that energy transfer between Chl *b* and Chl *a* occurs entirely within the monomeric subunits. However, there are some pronounced differences in the transfer kinetics of the monomeric and trimeric preparations which must be ascribed to the loss of some chlorophyll.

MATERIALS AND METHODS

Trimeric LHCII was prepared and purified from spinach using the method described earlier (*7*), starting with BBY membrane fragments (*23*) from spinach, based on anion-exchange chromatography and using the detergent *n*-dodecyl β,D-maltoside (DM) for solubilization of the complexes. Monomeric LHCII was obtained by incubation of trimers with 1% (w/v) octyl glucoside and 10 μg/mL phospholipase A_2 (plA_2) (Sigma) (*11*). Free pigments and some remaining trimers were removed by sucrose gradient (5−20% w/v) centrifugation (overnight at 40 000 rpm). For the absorption measurements the monomers were further purified with a Mono-Q anion-exchange FPLC (Pharmacia) to remove free pigments. For the measurements LHCII monomers and trimers were diluted in a buffer containing 20 mM Hepes (pH 7.5), 0.06% (w/v) DM, and 70% (v/v) glycerol. All measurements were performed at 77 K in a nitrogen bath cryostat (Oxford Instruments DN 1704). A cuvette with a path length of 0.2 cm was used.

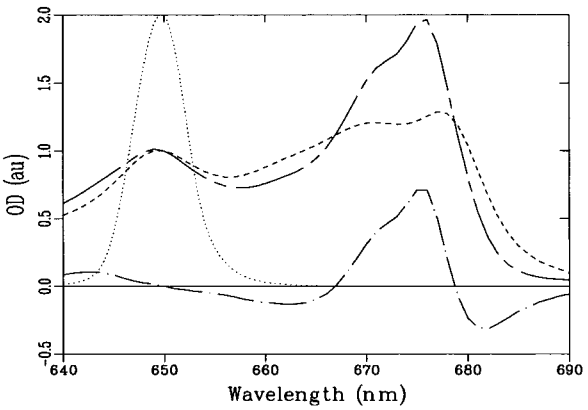

FIGURE 1: Absorption spectra at 77 K of monomers (- - -) and trimers (—-—) normalized at 650 nm, and the difference (—•—) of monomer and trimer absorption spectra. Also shown is the pump pulse centered at 650 nm (···).

Pump−probe measurements were performed using a 30 Hz laser system described in detail elsewhere (*12*, *24*). The system had an instrument response (cross correlation of pump and probe pulse) FWHM of 250−300 fs, which was modeled with a Gaussian. Excitation at 650 nm was achieved using a narrow band (6−7 nm FWHM) interference filter. The excitation energy of the pump beam was 0.3 μJ per pulse. The pump beam was focused with a 20 cm lens to a spot size of 250 μm in diameter (1×10^{15} photons/pulse/cm^2). The probe beam (spectral width 50 nm) was polarized under magic angle (54.7°) with respect to the pump beam.

The maximal absorption difference changes were $\lesssim$0.03 (OD 0.3 at 676 nm) for monomers and ~0.12 (OD 0.9 at 676 nm) for trimers at 676 nm. The monomer data set was measured up to a delay of ~670 ps, and the trimer data set was measured up to 40 ps (*12*). Measured spectra were analyzed in a global analysis routine, resulting in decay-associated difference spectra (DADS) and species-associated difference spectra (SADS) (*22*).

RESULTS

In Figure 1 the absorption spectra of LHCII monomers and trimers at 77 K and the difference spectrum are shown together with the excitation pulse centered at 650 nm. The spectra are normalized at 650 nm. Note that the normalization of the spectra is slightly arbitrary and the presented difference spectrum should be considered as an approximation of the true difference spectrum. The monomer spectrum (- - -) shows three different Chl *a* peaks: ~662, 670, and

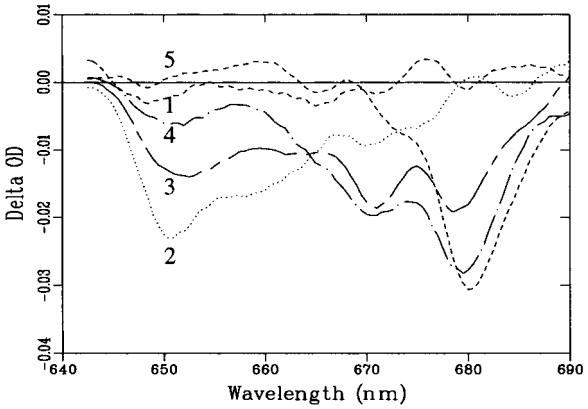

FIGURE 2: Absorption difference spectra (1−5) of LHCII monomers at 77 K measured at different delay times: before $t = 0$ (1) and at 0.3 ps (2), 0.6 ps (3), 1.7 ps (4), and 29 ps (5). Excitation wavelength is 650 nm.

678 nm. The trimer spectrum (—-—) shows a shoulder at 670 nm and a peak at 676 nm. The difference spectrum (—•—) clearly reflects a broadening of the monomer absorption spectrum compared to the trimer spectrum but also the loss of some Chl *a* absorption due to the loss of at least one Chl *a* per monomer (*2*). These effects are similar to those reported in (*11*).

Figure 2 shows some typical transient absorption difference spectra of the LHCII monomers after excitation at 650 nm. Plotted are absorption difference spectra obtained before $t = 0$ and after 0.3, 0.6, 1.7, and 29 ps. Several dynamic processes are immediately visible from the raw data. The bleaching/stimulated emission (SE) around 650 nm decays on a subpicosecond time scale concomitant with an increase of the bleaching/SE around 670 and 678 nm, reflecting energy transfer from Chl *b* to two different Chl *a* "pools". At 1.7 ps after the excitation pulse there are still some excitations localized on Chl *b*, pointing to some "slow" Chl *b* to Chl *a* transfer. Furthermore, a pronounced bleaching/SE signal at 670 nm is still visible. At 29 ps after the excitation pulse the bleaching/SE at 670 nm has mainly disappeared and the excitations are localized on the pigments showing bleaching/SE near 681 nm. Compared to the spectrum measured at a delay of 600 fs the bleaching/SE signal has shifted from 678 to 681 nm.

The total data set, containing 38 transient spectra up to a delay time of 670 ps, was analyzed using a global analysis routine (*22*). Four lifetimes were needed to get a satisfactory fit of the data: 200 fs, 3.2 ps, 18 ps, and 5.2 ns. The calculated DADS are shown in Figure 3A. The spectrum with the longest lifetime shows that the excitations become localized on the Chl *a* pigment(s) showing bleaching/SE at 680 nm. The lifetime of the longest-living component is not very accurate because the data set did not extend beyond 670 ps. The 200 fs process is clearly a transfer process from Chl *b* at 650 nm to Chl *a* pools showing bleaching/SE at 670 and 676 nm. Some of the bleaching/SE at 670 nm and 680 nm is due to a direct excitation of Chl *a*. Since the first lifetime of 200 fs was not very precise the amplitude of the first DADS is uncertain. The 3.2 ps spectrum represents energy transfer from Chl *b* absorbing near 650 nm to Chl *a* showing bleaching/SE slightly above 680 nm. With a time constant of 18 ps the bleaching/SE of the 670 nm pool disappears.

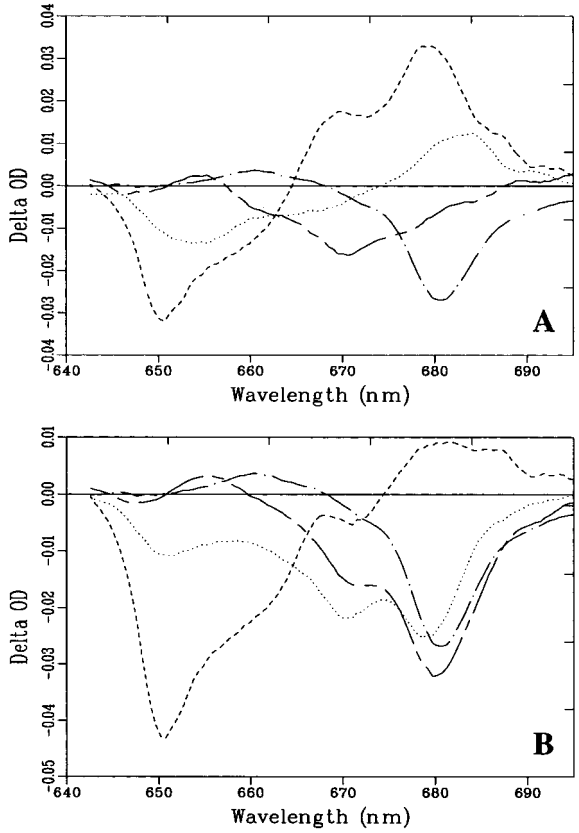

FIGURE 3: (A) DADS resulting from global analysis of the data of which a few spectra are shown in Figure 2. Time constants associated with these DADS: 200 fs (- - -), 3.2 ps (•••), 18 ps (—-—), and 5 ns (—•—). (B) SADS. (- - -) Initial bleaching from which the dotted spectrum (•••) is formed with a time constant of 200 fs. The dotted spectrum (•••) is replaced by the spectrum (—-—) with a time constant of 3.2 ps, and then with 18 ps the spectrum (—•—) is formed that decays with a time constant of 5 ns.

To show the time evolution of the spectra, the data are also fitted using a sequential model with increasing lifetimes, assuming transfer from one compartment to the next (A → B → C → D). We stress that this model is used merely to get a good description of the data, and the spectra should not be associated with real compartments. The unidirectionality is reasonable since at 77 K uphill energy transfer can be ignored. The SADS are characterized by the same time constants as the DADS. The spectra are shown in Figure 3B. The first SADS (dashed), which is the sum of the DADS, grows instantaneously with the pump pulse, it shows bleaching/SE of Chl *b* around 650 nm and some Chl *a* bleaching/SE at 670 nm due to direct excitation of Chl *a*. At even larger wavelengths a positive feature is visible, probably due to some excited-state absorption (ESA) which might interfere with bleaching/SE of directly excited Chl *a* molecules absorbing above 670 nm. The formation of the dotted spectrum (•••) is characterized by a time constant of 200 fs. It shows that the excitations are transferred very rapidly to pools showing bleaching/SE at 670 and 676 nm. Subsequently, the dotted spectrum is replaced by the chain dashed spectrum [(—-—), time constant 3.2 ps]. Clearly no Chl *b* bleaching/SE is visible any more while still a pronounced bleaching/SE at 670 is present. This bleaching/SE at 670 nm disappears with a time constant of 18 ps. Note also the appearance of some excited state absorption peaking at 655 nm. The long-living component that remains shows maximal bleaching/SE at 681 nm and the little shoulder at

670 nm is probably due to some unbound Chl *a*. Clearly visible is again the red shift of the maximal bleaching/SE signal in the red Chl *a* pool from 678 to 681 nm, probably reflecting equilibration. From the decrease of the total integrated signal it can be concluded that some annihilation has occured (see also Discussion).

DISCUSSION

How To Compare Monomers and Trimers?

In this work we have characterized the Chl *b* to Chl *a* singlet excitation transfer in monomeric LHCII. Specifically, we are interested whether the "slow" transfer between Chl *b* and Chl *a* with a time constant of several picoseconds occurs within or between monomeric subunits. This is of relevance, since the assignment of Chl *a* and Chl *b* molecules in the structural model of LHCII at 3.4 Å is not conclusive. In this model all Chl *b* molecules are in close contact to Chl *a* molecules within the same monomer and no major differences are expected for the Chl *b* to Chl *a* transfer times in monomers and trimers. However, significant differences in the kinetics would indicate a shortcoming of the proposed Chl assignment (*3*). Global analysis of the monomer data yielded time constants of 200 fs, 3.2 ps, 18 ps, and 5.2 ns, while global analysis of the trimer data gave time constants of 140 fs, 600 fs, 14 ps, and 700 ps (*12*). At this point is should be emphasized that even monomeric LHCII is a very complicated system of which the dynamics involves at least 12 components. These components cannot be resolved from the data. Given also the limited number of time-gated spectra (38 in this study) and the present signal to noise ratio, a certain decay time (τ) in the Chl *b* region is for instance not automatically related to an ingrowth of the bleaching in the Chl *a* region with exactly the same τ, and as a consequence the results of the global analysis depend on the wavelength region that is analyzed: it yields only the overall dominating processes when the entire spectrum (645−690 nm) is analyzed. Therefore, time constants resulting from a global analysis have a limited physical meaning and should be considered as the best way to characterize the dynamics. Therefore, a reasonable way to compare the (related) dynamics of LHCII trimers and monomers is to fit both data sets simultaneously since it is impossible to compare the spectral changes and the amplitudes of the different processes when these processes are expressed in different time constants.

Qualitative Comparison of Monomers and trimers

Prior to the simultaneous global analysis, the trimer ΔOD signal was scaled to the monomer ΔOD signal in the Chl *b* region at $t = 0.5$ ps. This time was chosen because that is just after the instrument response and the signals are not yet (strongly) affected by annihilation. Five components were needed to get a description of the monomer and trimer data in which all characteristic spectral changes could be retrieved. The use of additional components did not lead to a significant improvement of the fits. A satisfactory description of the data could be obtained using time constants of 140 fs, 600 fs, 8 ps, 20 ps, and 2.9 ns. These time constants should be seen as a "compromise" of the time constants resulting from separate fits of trimer and monomer data. The SADS are shown in Figure 4; not shown is the SADS at $t = 0$ because the uncertainty in the amplitude is too large in case of the trimers.

Figure 4A shows the SADS (dotted lines, monomers; dashed lines, trimers) after the 140 fs process has taken place. Monomer and trimer SADS show comparable amounts of Chl *b* bleaching/SE (640−658 nm) and Chl *a* bleaching/SE (658−690 nm), suggesting that a comparable amount of excitations has been transferred from Chl *b* to Chl *a*. However, in trimers the transferred excitations are concentrated more to the red with the bleaching/SE peaking close to 680 nm, while for the monomeric preparations more Chl *a* bleaching/SE is observed around 662 and 670 nm. As was already stated in the introduction, subpicosecond time constants must reflect energy transfer within a monomer or monomeric subunit. Thus, monomerization is not expected to influence the fast transfer processes and therefore we ascribe the differences between the monomer and trimer data to the loss of some Chl *a* and/or to the shift of the absorption spectrum of part of the Chl *a* molecules upon monomerization. These Chl *a* molecule(s) lead to bleaching/SE near 680 nm for trimeric preparations. Despite the absence or blue shift of these specific Chls *a*, the amount of transferred excitations from Chl *b* to Chl *a* within the instrument response time has remained unaltered. There are three obvious explanations for these findings.

(i) Part of the Chl *b* molecules can simultaneously transfer their energy ultrafast (within the instrument response time) to pigments giving rise to a signal near 680 nm (dominant fraction of transferred excitations) and to pigments giving rise to signals that are located more to the blue. The loss of the "680 nm pigments" now exclusively leads to transfer to the "blue" Chl *a* molecules from these specific Chl *b* molecules.

(ii) Part of the Chl *b* molecules transfer their excitations ultrafast to "blue" Chl *a* molecules which in turn transfer their excitations ultrafast to the "680 nm pigments". After the loss of the red pigments upon monomerization, the excitations are stuck on the "blue" Chl *a* molecules at least on this short time scale. Note that ultrafast transfer from the "blue" to the "red" part has indeed been observed for trimers (*12*).

(iii) Upon monomerization a "red" pigment becomes a "blue" pigment due to changes in the environment without strongly affecting the Chl *b* to Chl *a* transfer time.

At this stage we cannot discriminate between these possible explanations, but these observations should successfully be mimicked in future modeling of the spectroscopy and kinetics of LHCII.

In Figure 4B the spectrum is shown that is formed from the spectrum in Figure 4A with a time constant of 600 fs. Both monomers and trimers still show a limited amount of Chl *b* bleaching/SE. Again the Chl *a* 670 bleaching/SE is much more pronounced for monomers than for trimers.

With a time constant of 8 ps the spectra shown in Figure 4C are formed. The Chl *b* bleaching has disappeared for both monomers and trimers, and some excited state absorption becomes visible, peaking at 655 nm. In monomers clearly energy transfer has occurred from 670 to 679 nm. In trimers also transfer to the 679 nm pool has occurred but also some loss of bleaching/SE due to annihilation.

The spectra in Figure 4C are replaced by the spectra in Figure 4D with a time constant of 20 ps. The 670 nm shoulder in the spectrum of the trimers has completely

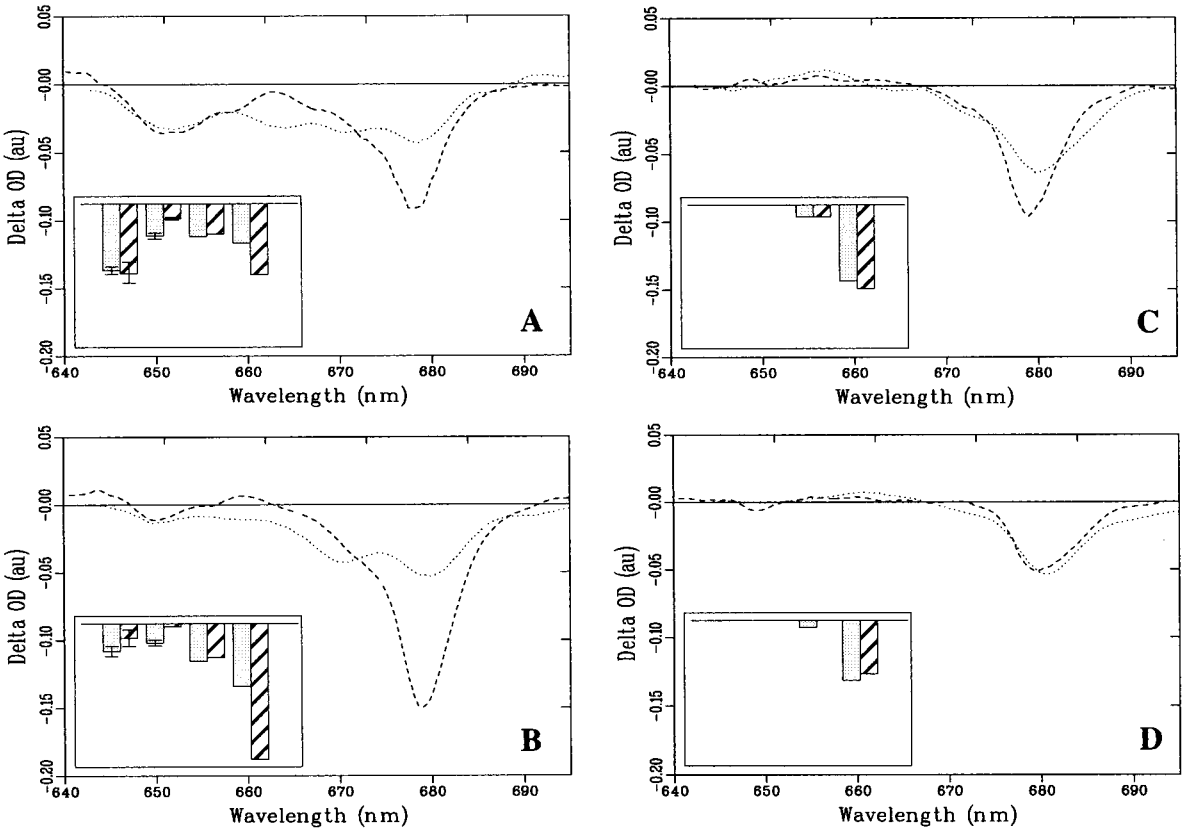

FIGURE 4: SADS, monomers (•••) and trimers (- - -), as calculated from a simultaneous fit of monomer and trimer data (77 K). (A) SADS, formed with a time constant of 140 fs, decaying with a time constant of 600 fs to form the SADS in B. (B) SADS decaying with a time constant of 8 ps, to form the SADS shown in C. (D) SADS decaying with a time constant of 20 ps, to form the SADS shown in D. (D) SADS decaying with a time constant of 2.9 ns. Bar diagrams (monomers, shaded; trimers, dashed) plotted in the insets of panels A−D are showing in which wavelength domains the excitations are localized. Bleaching/SE areas are measured and corrected for difference in extinction coefficient between Chl *a* and Chl *b*. The total wavelength domain is split in four parts: 640−658, 658−667, 667−675, and 675−690 nm. The size of the bar gives the relative amount of excitations in a certain domain, and the error bar shows the two possible extremes: no correction for excited state absorption, and maximal correction for excited state absorption (see text for further details).

disappeared. Monomers still show a small shoulder, probably due to unbound pigments. The area of the bleaching/SE of the trimers spectrum decreased more than the area of the monomer spectrum, indicating that more annihilation took place in the trimers.

Quantitative Comparison of Monomers and Trimers

To get a better view on the population changes in the different Chl pools the SA-spectra have been integrated in four different wavelength regions: 640−658, 658−667, 667−675, and 675−690 nm. Note that throughout the following discussion we neglect the influence of excitonic interactions. Although it was argued in (*12*, *25*) that the transfer from Chl *b* to Chl *a* can still be described by the Förster mechanism, these interactions might slightly influence the estimation of the amount of excitations localized on either Chl *a* and Chl *b*. The Chl *b* bleaching area (640−658 nm) is multiplied with a factor of 1.5 to correct for the difference between the extinction coefficients of Chl *a* and Chl *b*. Bar diagrams representing the obtained numbers are shown in the insets in Figure 4A−D. In the 640−658 and 658−667 nm regions a correction is made for the excited state absorption (error bars give extremes: no correction for ESA *vs* maximal correction for ESA, see below). Especially in the second component (Figure 4B) the estimation of the amount of Chl *b* bleaching strongly depends on the amount of excited-state absorption that has been taken into account.

As a next step we calculated the amplitudes of the different Chl *b* to Chl *a* transfer processes and we estimated the amount of Chl *b* bleaching/SE compared to the total bleaching/SE for each SA spectrum. A problem now is to decide which part of the spectrum is due to Chl *b* bleaching/SE and which part is due to Chl *a* bleaching/SE. To avoid a definitive choice we have split the spectra at different wavelengths: 658, 660, and 662 nm (see Table 2). As for the bar diagrams we have to correct for the different extinction coefficients of Chl *a* and Chl *b* and the excited state absorption of Chl *a* in the Chl *b* region. Errors are given again by the two extremes: no correction for ESA *vs* maximal correction for ESA. The ESA in Figure 4A and B was estimated by the ESA that is visible in the spectra in Figure 4C and D, multiplied by a factor correcting for the amount of 680 nm bleaching in the SA spectra of Figure 4A and B. Furthermore we estimated that 20% of the Chl *a* bleaching is due to direct excitation of Chl *a* (*12*). It was assumed that the Chl *b* absorption in the Chl *a* region can be neglected.

Table 2 shows the effect of the exact choice of the "splitting wavelength". In the previous estimates of the energy transfer amplitudes for the trimers we split the spectra at 662 nm, where the bleaching/SE is smallest (*12*). The appearance of bleaching/SE in the monomer data at this wavelength now led us to split the spectra also at 658 nm. In (*11*) it was argued that, in contradiction to (*9*), the 661

Table 2: Amplitudes of Chl *b* → Chl *a* Transfer Processes Estimated from the Integrated Areas of the SADS Shown in Figure 4; the "Splitting Wavelength" Is Varied (See Text)

sample	time constant (ps)	amplitudes (%) 640−658 (Chl *b*) 658−690 (Chl *a*)	640−660 (Chl *b*) 660−690 (Chl *a*)	640−662 (Chl *b*) 662−690 (Chl *a*)
monomers	0.14	50 ± 3	46 ± 3	38 ± 3
	0.6	27 ± 3	24 ± 3	30 ± 4
	8	23 ± 3	30 ± 3	32 ± 4
trimers	0.14	53 ± 5	50 ± 5	45 ± 5
	0.6	37 ± 5	37 ± 7	41 ± 7
	8	10 ± 5	13 ± 7	14 ± 7

nm band has to be assigned to Chl *a*, suggesting that it is more realistic to split at 658 nm. The trends are independent of the "splitting wavelength". The following discussion will be limited to the results that were found after splitting the spectra at 658 nm.

The ultrafast (140 fs) energy transfer from Chl *b* to Chl *a* has an amplitude of ∼50% (2.5−3 Chl *b* pigments) for both monomers and trimers. However, the amplitudes of the intermediate and slow components differ from monomers and trimers. For monomers these processes have comparable amplitudes, 27 ± 3% and 23 ± 3%, respectively, while for trimers the intermediate process has a larger amplitude than the slow process: 37 ± 5% and 10 ± 5%. This suggests that for monomers ∼0.8 ± 0.5 Chl *b* transfers its energy more slowly (changed from ∼600 fs in trimers to several picoseconds in monomers), assuming that every Chl *b* has an equal probability to be excited, and that in total 5−6 Chl *b* pigments are bound to the protein.

As was stated in the introduction, the 600 fs process should be ascribed to intramonomeric transfer (from Chl *b* to Chl *a*). Therefore, we also conclude for this change that it is due to the loss of some Chl *a*. Since 1−2 Chl *a* molecules are lost upon monomerization (*2*), we cannot conclude whether this is the same "680 nm pigment" that caused the reduction of the ultrafast energy transfer (within instrument response time) to the red part of the LHCII absorption (see above). Also this observed decrease in the transfer rate for approximately 1 Chl *b* molecule is of possible use for future modeling studies.

As mentioned above part of this study was motivated to investigate whether the "slow" transfer process (several picoseconds) from Chl *b* to Chl *a* occurs within or between monomeric subunits. It can be concluded from the present analysis that the slowest Chl *b* to Chl *a* transfer has not significantly slowed down in monomers, demonstrating that it is due to transfer within a monomer. If it would have been due to transfer between different monomeric subunits the observed time would have considerably slowed down upon monomerization. Therefore, the present results are in line with the assignment of the chlorophyll molecules by Kühlbrandt, Wang, and Fujiyoshi (*3*) although the results do not prove that the assignment is correct.

Annihilation

As was already stated above, annihilation occurs on all timescales and will probably influence each component of the global analysis. The question now is how large is the influence of the annihilation on the detected kinetics? Annihilation at early times is not very likely since then Chl *b* to Chl *a* transfer occurs mainly between nearby molecules. The probability to excite simultaneously both molecules of such a Chl *a*−Chl *b* pair is not very high. For the same reason fast Chl *b* to Chl *b* annihilation is not very likely. At later times, when all excitations are on Chl *a*, this annihilation is more probable, since it can take place over larger distances. In Table 3 we listed the integrated areas of the bleaching/SE for the different SADS. In parallel with the transfer process described by the 600 fs time constant annihilation occurs and its amplitude is at most 15%. Annihilation becomes more important on timescales longer than 1 ps. If annihilation would only occur between Chl *a* molecules we might have overestimated the relative amount of excitations on Chl *b* because we normalized on the total bleached area. However, this would increase the contribution of the intermediate component (600 fs) only slightly from 27% to 30% and decrease that of the slow component from 23% to 20%. In addition, comparison of our data for trimeric LHCII (*12*) with the annihilation free measurements by Connelly and co-workers (*13*) show very similar time constants and amplitudes. Therefore we conclude that annihilation does not disturb our measurements and the conclusion to a significant extent.

Table 3: Number of Excitations, Estimated from the SADS in Figure 4, in Which the SADS in Figure 4A Are Normalized to 1 (See Text for Details)

sample	area SADS 4A	SADS 4B	SADS 4C	SADS 4D
monomers	1	0.85 ± 0.03	0.5	0.4
trimers	1	0.94 ± 0.04	0.5	0.3

CONCLUSIONS

In this study we measured the Chl *b* to Chl *a* energy transfer in monomers of LHCII using transient absorption measurements. Four components were needed in the global analysis to get a satisfactory description of the data: 200 fs, 3 ps, 18 ps, and 5 ns. The first two components reflect transfer process from Chl *b* to Chl *a*. The 18 ps component can be associated with a transfer process from a 670 nm Chl *a* pool to a 680 nm Chl *a* pool although the time constant is probably somewhat influenced by annihilation.

For comparison the monomer data have been fitted simultaneously with previous (*12*) LHCII trimer data. We have shown that the ultrafast (fitted here with a 140 fs component) Chl *b* to Chl *a* energy transfer has an amplitude of ∼50% both for monomers and trimers. This transfer occurs to pigments that are, on the average, absorbing significantly more to the blue in the case of monomers. It is possible that the absorption of one or several Chl *a* molecules has shifted to the blue in monomers compared to trimers. However, the difference can also be due to the fact that some

Chl *a* was lost upon monomerization. The amount of energy transfer that occurs with a time constant of 600 fs has been diminished at the expense of the occurrence of a process that takes place with a time constant of several picoseconds and quantitative analysis suggests that 0.8 ± 0.5 Chl *b* transfers slower in monomers than in trimers. Also this change must be due to the loss of some Chl *a*. Finally, we conclude that all energy transfer from Chl *b* to Chl *a* takes place within the monomeric subunits of LHCII, in line with the model proposed by Kühlbrandt and co-workers (*3*).

REFERENCES

1. Van Grondelle, R., Dekker, J. P., Gillbro, T., and Sundström, V. (1994) *Biochim. Biophys. Acta 1187*, 1−65.
2. Peterman, E. J. G., Gradinaru, C. C., Calkoen, F., Borst, C. J., van Grondelle, R., and van Amerongen, H. (1997) *Biochemistry 36*, 12208−12215.
3. Kühlbrandt, W., Wang, D. N., and Fujiyoshi, Y. (1994) *Nature 367*, 614−621.
4. Frank, H. A., and Cogdell, R. J. (1996) *Photochem. Photobiol. 63*, 257−264.
5. Van der Vos, R., Carbonera, D., and Hoff, A. J. (1991) *Appl. Magn. Reson. 2*, 179−202.
6. Carbonera, D., and Giacometti, G. (1992) *Rend. Fis. Acc. Lincci 3*, 361−368.
7. Peterman, E. J. G., Dukker, F. M., van Grondelle, R., and van Amerongen, H. (1995) *Biophys. J. 69*, 2670−2678.
8. Hemelrijk, P. W., Kwa, S. L. S., van Grondelle, R., and Dekker, J. P. (1992) *Biochim. Biophys. Acta 1098*, 159−166.
9. Krawczyk, S., Krupa, Z., and Maksymiec, W. (1993) *Biochim. Biophys. Acta 1143*, 273−281.
10. Savikhin, S., van Amerongen, H., Kwa, S. L. S., van Grondelle, R., and Struve, W. S. (1994) *Biophys. J. 66*, 1597−1603.
11. Nussberger, S., Dekker, J. P., Kühlbrandt, W., van Bolhuis, B. M., van Grondelle, R., and van Amerongen, H. (1994) *Biochemistry 33*, 14775−14783.
12. (a) Visser, H. M., Kleima, F. J., van Stokkum, I. H. M., van Grondelle, R., and van Amerongen, H. (1996) *Chem. Phys. 210*, 297−312. (b) Visser, H. M., Kleima, F. J., van Stokkum, I. H. M., van Grondelle, R., and van Amerongen, H. (1997) *Chem. Phys. 215*, 299.
13. Connelly, J. P., Müller, M. G., Hucke, M., Gatzen, G., Mullineaux, C. W., Ruban, A. V., Horton, P., and Holtzwarth, A. R. (1997) *J. Phys. Chem. B 101*, 1902−1909.
14. Peterman, E. J. G., Monshouwer, R., van Stokkum, I. H. M., van Grondelle, R., and van Amerongen, H. (1997) *Chem. Phys. Lett. 264*, 279−284.
15. Bittner, T., Irrgang, K.-D., Renger, G., and Wasielewski, M. (1994) *J. Phys. Chem. 98*, 11821−11826.
16. Bittner, T., Wiederrecht, G. P., Irrgang, K.-D., Renger, G., and Wasielewski, M. (1995) *Chem. Phys. 194*, 311−322.
17. Du, M., Xie, X., Mets. L., and Fleming, G. R. (1994) *J. Phys. Chem. 98*, 4736−4741.
18. Pålsson, L. O., Sprangfort, M. D., Gulbinas, V., and Gilbro, T. (1994) *FEBS Lett. 339*, 134−138.
19. Eads, D. D., Castner, E. W., Alberte, R. S., Mets, L., and Fleming, G. R. (1989) *J. Phys. Chem. 93*, 8271−8275.
20. Mullineaux, C. W., Pascal, A. A., Horton, P., and Holzwarth, A. R. (1993) *Biochim. Biophys. Acta 1141*, 23−28.
21. Kwa, S. L. S., van Amerongen, H., Lin, S., Dekker, J. P., van Grondelle, R., and Struve, W. S. (1992) *Biochim. Biophys. Acta 1101*, 202−212.
22. Van Stokkum, I. H. M., Scherer, T., Brouwer, A. M., and Verhoeven, J. W. (1994) *J. Phys. Chem. 98*, 852−866.
23. Berthold, D. A., Babcock, G. T., and Yocum, C. F. (1981) *FEBS Lett. 134*, 231−234.
24. Visser, H. M., Groot, M.-L., van Mourik, F., van Stokkum, I. H. M., Dekker, J. P., and van Grondelle, R. (1995) *J. Phys. Chem. 99*, 15304−15309.
25. Trinkunas, G., Connelly, J. P., Müller, M. G., Valkunas, L., and Holzwarth, A. R. (1997) *J. Phys. Chem. B. 101*, 7313−7320.

BI9716480